Acta Neuropathologica Communications

RESEARCH

Open Access

Protein phosphatase 2Cm-regulated branched-chain amino acid catabolic defect in dorsal root ganglion neurons drives pain sensitization

Nan Lian[1,2†], Fangzhou Li[3,4†], Cheng Zhou[3], Yan Yin[5], Yi Kang[3], Kaiteng Luo[1,3,4], Su Lui[2], Tao Li[1,3,6*] and Peilin Lu[1,3,4,6*]

Abstract

Maladaptive changes of metabolic patterns in the lumbar dorsal root ganglion (DRG) are critical for nociceptive hypersensitivity genesis. The accumulation of branched-chain amino acids (BCAAs) in DRG has been implicated in mechanical allodynia and thermal hyperalgesia, but the exact mechanism is not fully understood. This study aimed to explore how BCAA catabolism in DRG modulates pain sensitization. Wildtype male mice were fed a high-fat diet (HFD) for 8 weeks. Adult $PP2Cm^{fl/fl}$ mice of both sexes were intrathecally injected with pAAV9-hSyn-Cre to delete the mitochondrial targeted 2 C-type serine/threonine protein phosphatase (PP2Cm) in DRG neurons. Here, we reported that BCAA catabolism was impaired in the lumbar 4–5 (L4-L5) DRGs of mice fed a high-fat diet (HFD). Conditional deletion of PP2Cm in DRG neurons led to mechanical allodynia, heat and cold hyperalgesia. Mechanistically, the genetic knockout of PP2Cm resulted in the upregulation of C-C chemokine ligand 5/C-C chemokine receptor 5 (CCL5/CCR5) axis and an increase in transient receptor potential ankyrin 1 (TRPA1) expression. Blocking the CCL5/CCR5 signaling or TRPA1 alleviated pain behaviors induced by PP2Cm deletion. Thus, targeting BCAA catabolism in DRG neurons may be a potential management strategy for pain sensitization.

Keywords BCAAs, DRG, Pain sensitization, CCL5/CCR5 axis, TRPA1

†Nan Lian and Fangzhou Li contributed equally to this work as first authors.

†Tao Li and Peilin Lu contributed equally to this work as corresponding authors.

*Correspondence:
Tao Li
scutaoli1981@scu.edu.cn
Peilin Lu
peilinlyu@qq.com
[1]Laboratory of Mitochondria and Metabolism, West China Hospital of Sichuan University, Chengdu 610041, China
[2]Huaxi MR Research Center (HMRRC), Department of Radiology, Functional and Molecular Imaging Key Laboratory of Sichuan Province, West China Hospital of Sichuan University, Chengdu 610041, China
[3]Department of Anesthesiology, National-Local Joint Engineering Research Centre of Translational Medicine of Anesthesiology, West China Hospital of Sichuan University, Chengdu 610041, China
[4]Department of Anesthesiology, West China Hospital of Sichuan University, Chengdu 610041, China
[5]Department of Pain Management, West China Hospital of Sichuan University, Chengdu 610041, China
[6]West China Hospital, Sichuan University, No 37 Wainan Guoxue Road, Chengdu 610041, Sichuan, China

Introduction

Peripheral pain hypersensitivity is characterized by decreased sensory thresholds, increased responsiveness to stimuli, and allodynia, in which normally innocuous stimuli are perceived as painful [1, 5]. Persistent pain hypersensitivity causes distress to humans, interfering with physical and mental activities [30]. Current treatments for this disorder have a modest effect, primarily due to the inability to precisely target the underlying mechanisms. Altered metabolic states in the primary sensory neurons of dorsal root ganglion (DRG) have been shown to induce abnormal signal transduction and gene expression, resulting in persistent pain hypersensitivity [7]. Therefore, understanding the etiology of metabolic dysfunctions in the DRG may prompt novel therapeutic treatments for pain hypersensitivity.

Branched-chain amino acids (BCAAs), including leucine, isoleucine, and valine, are indispensable nutrients for human beings. Aberrant BCAA catabolism has been implicated in the pathogenesis of diabetes, and one-third of patients develop neuropathic pain [3, 4, 25]. In previous study, we have reported that obesity-induced pain hypersensitivity is coupled with an accumulation of BCAAs in lumbar DRG due to BCAA catabolism deficiency [15], supporting a link between defective BCAA catabolism and pain sensitization. However, whether BCAA homeostasis in the DRG regulates pain behaviors and underlying molecular mechanisms remain elusive.

Defective BCAA catabolism promotes the release of proinflammatory molecules, contributing to the development and persistence of pain hypersensitivity [46]. C-C chemokine ligand 5 (CCL5), also called RANTES, is a small secreted protein that acts as an important proinflammatory mediator in the pathogenesis of neuropathic pain [20]. CCL5 directly excites DRG neurons by activating its preferred C-C chemokine receptor 5 (CCR5) [43]. Studies have showed that intrathecal administration of CCL5 produces mechanical allodynia and thermal hyperalgesia, and treatment with CCL5-neutralizing antibodies or CCR5 antagonists alleviates pain behaviors in different pain models [11, 16, 17, 47]. Thus, the CCL5/CCR5 signaling axis in the DRG may be a critical mediator of pain hypersensitivity due to defective BCAA catabolism.

The transient receptor potential ankyrin 1 (TRPA1) channel is a pain sensor that responds to irritating chemicals, noxious mechanical, cold, and heat stimuli, and can be sensitized by endogenous proinflammatory agents [18, 45]. It is primarily localized to a subpopulation of primary sensory neurons in the DRG [33]. Animals lacking TRPA1 expression or treated with TRPA1 antagonists exhibit reduced nociceptive behaviors upon exposure to noxious stimuli [28]. However, the specific role of TRPA1 in pain manifestation induced by BCAA catabolic defect remains unclear.

The BCAA catabolic enzyme, mitochondrial targeted 2 C-type serine/threonine protein phosphatase (PP2Cm), is highly expressed in the brain and DRG, mainly in all neuronal subtypes [13, 37, 48]. Genetic deletion of PP2Cm impairs BCAA catabolism, leading to increased BCAA levels [14, 40]. In this study, we observed that conditional knockout of PP2Cm in DRG neurons resulted in pain hypersensitivity, and further investigated how defective BCAA catabolism modulates pain behaviors. Our results suggest that targeting BCAA catabolism in DRG sensory neurons may be a novel therapeutic strategy for pain sensitization.

Materials and methods

Animals

All procedures were approved by the Animal Ethics Committee of West China Hospital, Sichuan University, China (Protocol No.20230310052), and the protocols were performed under strict adherence to the Animal Research: Reporting of in vivo Experiments (ARRIVE) guidelines. Animals received humane care in accordance with the Guide for the Care and Use of Laboratory Animals published by the NIH. Wild-type C57BL/6J mice were purchased from Vital River Laboratory Animal Technology Co. Ltd. (Beijing, China). The mice were housed in a conventional facility at 22±2 °C under a 12 h light-dark cycle with free access to food and water.

Male C57BL/6J mice (~4 weeks of age, weighed 13–15 g) were randomly fed a high-fat diet (HFD) composed of 60% kcal per kg fat (D12492, Research Diets Inc, New Brunswick, NJ, USA), or a chow diet (CD) composed of 11.85% kcal per kg fat (SWC9101, Xietong Ltd., Nanjing, China) for 8 weeks. Body weight and nonfasting blood glucose levels were recorded weekly. PP2Cm$^{fl/fl}$ mice on a C57BL/6J background were purchased from Cyagen Biosciences Inc. (Guangzhou, China) and bred to produce littermates. Adult PP2Cm$^{fl/fl}$ mice (~8 weeks of age, weighed 20–25 g) of both sexes were intrathecally injected with 5 μL of pAAV9-hSyn-Cre (3×10^{13} VG/mL) to generate PP2Cm-cKO mice. Control mice (PP2Cm-ctrl) received the same volume of pAAV9-hSyn vector (Vigenebio, Jinan, China). After 3 weeks, the efficiency of PP2Cm deletion in DRG was validated using Western blotting analysis. The mice were randomly assigned to different groups. The experimenters were blinded to the group assignments and treatment conditions. At the end of the experimental protocol, the mice were anesthetized with 2% isoflurane and sacrificed to collect the bilateral lumbar 4–5 (L4-L5) DRGs.

Behavioral testing

On each testing day, the assay order was randomized, and experiments were carried out by blinded observers. Prior to testing, the mice were acclimated to the environment.

Mechanical, thermal, and cold sensitivity tests were conducted at 30- to 60-minute intervals, allowing the mice to return to their home cages with access to food and water.

In the von Frey test [44], the mice were placed in an individual Plexiglas chamber on an elevated mesh grid floor. After 1-hour acclimation period, the mechanical paw withdrawal thresholds were assessed using von Frey filaments with an ascending order (mice: 0.008, 0.02, 0.04, 0.07, 0.16, 0.4, 0.6, 1.0, and 1.4 g). Each filament was applied 5 times to the mid-plantar surface of hind paws for 5 s with a 30 s interval, starting with 0.008 g and ending with 1.4 g force. Abrupt paw raising, retracting, or licking was considered as a positive response. The absolute withdrawal thresholds were determined by the up-down method [27].

In the Hargreaves test [44], paw withdrawal latencies in response to thermal stimulation were examined with a radiant heat source (Model 37370; Ugo-Basile). In a quiet room, the mice were placed in a transparent chamber on a glass plate. After the mice adapted to the environment, the plantar surface of hind paws was stimulated with a radiant heat beam (IR=35 mW/cm^2). When the hind paws were moved, the light source automatically turned off, and the withdrawal latencies were recorded. Measurements were repeated 3 times with a 10-min interval. The average latencies were calculated. To avoid damage to the hind paws, a cutoff time of 20 s was used.

In the cold plate test [2], the mice were placed on a cold plate apparatus (Bioseb) set at 4 ˚C. Paw withdrawal latencies were defined as the time at which a positive response occurred (e.g., jumping, shaking, or licking of the feet). Measurements were repeated 3 times within a 10-min interval. A cutoff time of 50 s was applied to avoid potential tissue damage. Mice showing no response within 50 s were removed from the apparatus, and the time was recorded as 50 s.

Drugs and intrathecal injection

Compound BT2 (3,6-dichlorobenzo[b]thiophene-2-carboxylic acid, sc-276559, Santa Cruz Biotechnology), an inhibitor of BCKDK, was diluted in the vehicle (5% DMSO, 10% cremophor EL, and 85% 0.1 M sodium bicarbonate, pH 9.0) and administered via oral gavage at a dose of 40 mg/kg body weight per day. A mouse neutralizing antibody for CCL5 (anti-CCL5, AF478-SP, R&D Systems) was reconstituted in saline and intrathecally injected at a dose of 2.5 μg/mouse in a volume of 5 μL, for 2 consecutive days [19]. The CCR5 specific antagonist maraviroc (M1971, AbMole) was dissolved in sterile DMSO and diluted with saline for single intrathecal (i.t.) injection at a dosage of 40 μg/mouse in 5 μL volume [12]. The TRPA1-selective antagonist Chembridge-5861528 (Chem-5861528, M7387, AbMole) was dissolved in sterile DMSO and diluted with saline for 20 μg/5 μL/mouse i.t. injection [34, 35]. Normal IgG and saline were used as controls. The *Ccr5*-directed small interfering RNA (siCcr5, sense: 5'-CAGUAGUUCUAAUAGACUATT-3'; antisense: 5'-UAGUCUAUUAGAACUACUGTT-3'), *Trpa1*-directed small interfering RNA (siTrpa1, sense: 5'-GCUAAGCUGUGUAAAUCAATT-3'; antisense: 5'-UUGAUUUACACAGCUUAGCTT-3'), and control small interfering RNA (siCtrl, sense: 5'-UUCUCCGAACGUGUCACGUdTdT-3'; antisense: 5'-ACGUGACACGUUCGGAGAAdTdT-3') (Vigenebio, Jinan, China) were dissolved in RNase-free water and administered intrathecally at 2 μg/μL in a volume of 5 μL.

Measurement of branched-chain amino acid concentrations

Fresh bilateral L4-L5 DRG tissues from CD and HFD mice, PP2Cm-cKO and PP2Cm-ctrl mice, PP2Cm-cKO+Vehicle and PP2Cm-cKO+BT2 mice, were collected for subsequent BCAA concentration analysis. DRG tissue samples were homogenized in sterile water and mixed with equal volumes of acetonitrile. After centrifugation (at 15000 × g, 4 °C, for 10 min), the supernatant was collected and diluted for the detection of BCAA concentrations by liquid chromatography-tandem mass spectrometry (LC-MS, 1260–6460, Agilent).

Chromatographic separation was performed using a InfinityLab Poroshell HPH-C18 column (4.6×100 mm, 2.7 μm, Part no. 695975-702, Agilent), and involved isocratic condition with a flow rate of 0.3 mL/min and an injection volume of 1 μL. The column temperature was maintained at 30 °C. Mobile phase composition was 0.1% formic acid aqueous solution and acetonitrile (v/v=95:5). Mass spectrometric acquisition was performed in the positive mode of electrospray ionization (ESI), with source temperature of 350 °C and capillary voltage of 3500 V. Multiple reaction monitoring (MRM) was employed as the scan mode. Standard chemicals, L-leucine, L-isoleucine, and L-valine (Sigma-Aldrich) were used to quantify their concentrations. A series of calibration standards were analyzed to generate concentration-response curves over a dynamic range. Three models were established using linear regression to back-calculate the concentrations of leucine, isoleucine, and valine in samples, respectively. The parameters of fragmentor, mass-to-charge ratio (m/z), and collision energy, as well as representative LC-MS traces in blank, standard, and sample, have been provided in Supplementary Fig S1.

RNA sequencing

Bilateral L4-L5 DRG tissues from 9 mice per group were excised for RNA sequencing (RNA-seq). Then, the DRGs from 3 mice were pooled into each sample. Total RNA was isolated using the TRIzol Reagent (15596026CN, Invitrogen/ThermoFisher Scientific), after which the

concentration, quality, and integrity were determined using a NanoDrop spectrophotometer (701-058112, ThermoFisher Scientific). Three micrograms of RNA were used for RNA sample preparation. mRNA was purified from the total RNA using poly-T oligo-attached magnetic beads. Fragmentation was carried out using divalent cations at elevated temperature in Illumina's proprietary buffer. Sequencing libraries were constructed with the VAHTS Universal V10 RNA-seq Library Prep Kit for Illumina (NR606, Vazyme). The insert size for final cDNA library was 300–400 bp. We then performed 2×150 bp paired-end sequencing on the Illumina NovaSeq™ 6000 platform (Personal Biotechnology Co., Ltd., Shanghai, China) following the manufacturer's recommended protocol. We obtained raw read counts on each gene of each sample and standardized gene expression using fragments per kilobase of transcript per million mapped reads (FPKM) method. Volcano plot, cluster heatmap, and Kyoto Encyclopedia of Genes and Genomes (KEGG) pathway enrichment analyses were conducted on Personalbio gene clouds under the following screening criteria: expression fold change > 1.5 and significant p value < 0.05.

Quantitative real-time PCR

Total RNA was isolated from frozen DRG tissues using TRIzol Reagent (15596026CN, Invitrogen/ThermoFisher Scientific), and cDNA was synthesized using iScript cDNA Synthesis Kit (170–8891, Bio-Rad). Quantitative PCR (qPCR) was performed using iTaq Universal SYBR Green Supermix (1725124, Bio-Rad) with template cDNA and primers for each gene in a Bio-Rad CFX96 real-time PCR system. The relative fold change in mRNA expression was calculated with the $2^{-\Delta\Delta Ct}$ method with *β-actin* as the internal control. The primer sequences were listed in Supplementary Table S1.

Western blotting assay

Frozen DRG tissues were lysed with RIPA buffer supplemented with a protease inhibitor cocktail (4693116001, Roche), PMSF and Na_2VO_3. Protein samples (20–120 μg) were separated by SDS–PAGE and transferred onto PVDF membranes. The blots were blocked in 5% nonfat milk and incubated at 4 °C overnight with primary antibodies, including anti-PP2Cm (1:1000, DF4348, Affinity Biosciences), anti-CCR5 (1:1000, AF6339, Affinity Biosciences), anti-TRPA1 (1:1000, 19124-1-AP, Proteintech), anti-α-tubulin (1:5000, AF0524, Affinity Biosciences) and anti-GAPDH (1:5000, AF7021, Affinity Biosciences). After incubation with secondary antibody (1:10000, RGAR001, Proteintech) for 1 h at room temperature, the signals were visualized by a Novex™ ECL Chemiluminescent Substrate Reagent Kit (WP20005, ThermoFisher Scientific) and exposed using ChemiDoc XRS system (Bio-Rad) with Image Lab software. The band intensities were quantified with Image J software.

CCL5 enzyme-linked immunosorbent assay (ELISA)

DRG tissues were rapidly dissected and homogenized in 100 μL of DPBS containing protease inhibitors. The homogenate supernatants were isolated by centrifugation at 4000 × g for 10 min. CCL5 levels in the L4-L5 DRGs were measured using an ELISA kit (E-EL-M0009, Elabscience) according to the manufacturer's protocol.

Immunohistochemistry

Mice were deeply anesthetized with 2% isoflurane and then transcardially perfused with phosphate buffered saline (PBS, pH 7.4) for 5 min, followed by 4% paraformaldehyde until muscle twitching stopped. The L4-L5 DRGs were fixed in 4% paraformaldehyde, followed by dehydration in an ascending ethanol series. Tissues were embedded in paraffin and cut into 5 μm sections for immunofluorescence staining. The sections were incubated at 4 °C overnight with the following primary antibodies: PP2Cm (1:100, DF4348, Affinity Biosciences), CCR5 (1:100, AF6339, Affinity Biosciences), TRPA1 (1:100, DF13269, Affinity Biosciences), Neurofilament 200 (NF200, 1:100, N0142, Sigma Aldrich), CGRP (1:100, ab81887, Abcam), and IB_4 Alexa Fluor 488 (5 μg/μL, I21411, ThermoFisher Scientific). The sections, except for slices incubated with IB_4 Alexa Fluor 488 antibodies, were incubated with Alexa Fluor 488 goat anti-mouse IgG (1:400, ab150113, Abcam), or Fluor 594 goat anti-rabbit IgG (1:400, ab150080, Abcam) secondary antibody for 2 h. Fluorescence images were acquired by Olympus (VS200, Tokyo, Japan), and analysis was performed blindly on three sections per DRG using OlyVIA digital software and ImageJ software.

Statistical analysis

Statistical analysis was performed with GraphPad Prism 8 software. All data were presented as the mean ± SEM unless otherwise stated. The intensities of the protein bands and immunofluorescence were quantified using ImageJ software. Body weight, nonfasting blood glucose levels, the behavioral thresholds in CD and HFD-fed mice, as well as in PP2Cm-ctrl and PP2Cm-cKO mice, fold changes in mRNA expression of *Ccl5*, *Ccr5*, *Il-1β*, *Tnf-α*, *Trpa1*, and *Trpv1*, CCL5 levels, and the immunofluorescence intensity were analyzed with two-tailed unpaired Student's t-tests. BCAA levels, the fold changes in BCAA catabolic enzymes, and behavioral time course data for anti-CCL5, maraviroc, siCcr5, Chem-5,861,528 and siTrpa1 treatment in PP2Cm-cKO mice were analyzed with two-way repeated measures analysis of variance (ANOVA) with Bonferroni posttests to determine the significance of differences between groups at each

individual time point. CCL5 levels after anti-CCL5 treatment, *Ccr5* mRNA levels after siCcr5 injection, and *Trpa1* mRNA levels after siCcr5 and siTrpa1 injection were analyzed with one-way ANOVA with Tukey's multiple comparisons test. Differences were considered significant when $P<0.05$.

Results

The catabolism of branched-chain amino acids is impaired in the lumbar 4–5 dorsal root ganglia of HFD-fed mice

Four-week-old male mice were fed with a standard chow diet (CD) or high-fat diet (HFD) for 8 weeks, as shown in Fig. 1a. Consistent with a previous study [15], mice fed a HFD for 8 weeks showed increased body weight and nonfasting blood glucose levels (Fig. 1b, c; body weight $p<0.0001$, nonfasting blood glucose levels $p=0.0002$). After 8-week HFD, male mice exhibited mechanical allodynia and heat hyperalgesia, but no cold hyperalgesia (Fig. 1d-f; mechanical thresholds $p<0.0001$, heat latencies $p=0.0005$, cold latencies $p=0.10$). Furthermore, these mice showed an accumulation of BCAAs in the L4-L5 DRGs, along with significant decrease in the relevant catabolic enzymes – *Bcat2* by approximately 44%, and *Pp2cm* by ~37%, and a ~1.47-fold increase in *Bckdk* (Fig. 1g, h; leucine $p=0.02$, isoleucine $p=0.67$, valine $p=0.001$; *Bcat1* $p=0.07$, *Bcat2* $p=0.006$, *Bckdha* $p=0.05$, *Bckdhb* $p=0.17$, *Pp2cm* $p=0.03$, *Bckdk* $p=0.02$). Collectively, our results indicate impaired BCAA catabolism in the L4-L5 DRGs of HFD-fed mice, which exhibit hyperalgesic phenotypes.

Conditional knockout of PP2Cm in DRG neurons leads to pain hypersensitivity

Next, we investigated whether impaired BCAA catabolism in the L4-L5 DRGs contributed to the development of pain sensitization. PP2Cm, which regulates the rate limiting step of BCAA degradation, was knocked out to impair BCAA catabolism. To delete PP2Cm in DRG neurons, pAAV9-hSyn-Cre or pAAV9-hSyn was intrathecally injected into the subarachnoid space of male and female $PP2Cm^{fl/fl}$ mice to generate conditional knockout (PP2Cm-cKO) and control (PP2Cm-ctrl) mice, respectively (Fig. 2a). The efficiency of PP2Cm knockout was confirmed on day 21 post-injection. PP2Cm protein expression in the L4-L5 DRGs of PP2Cm-cKO mice was reduced by ~80% compared to PP2Cm-ctrl mice of

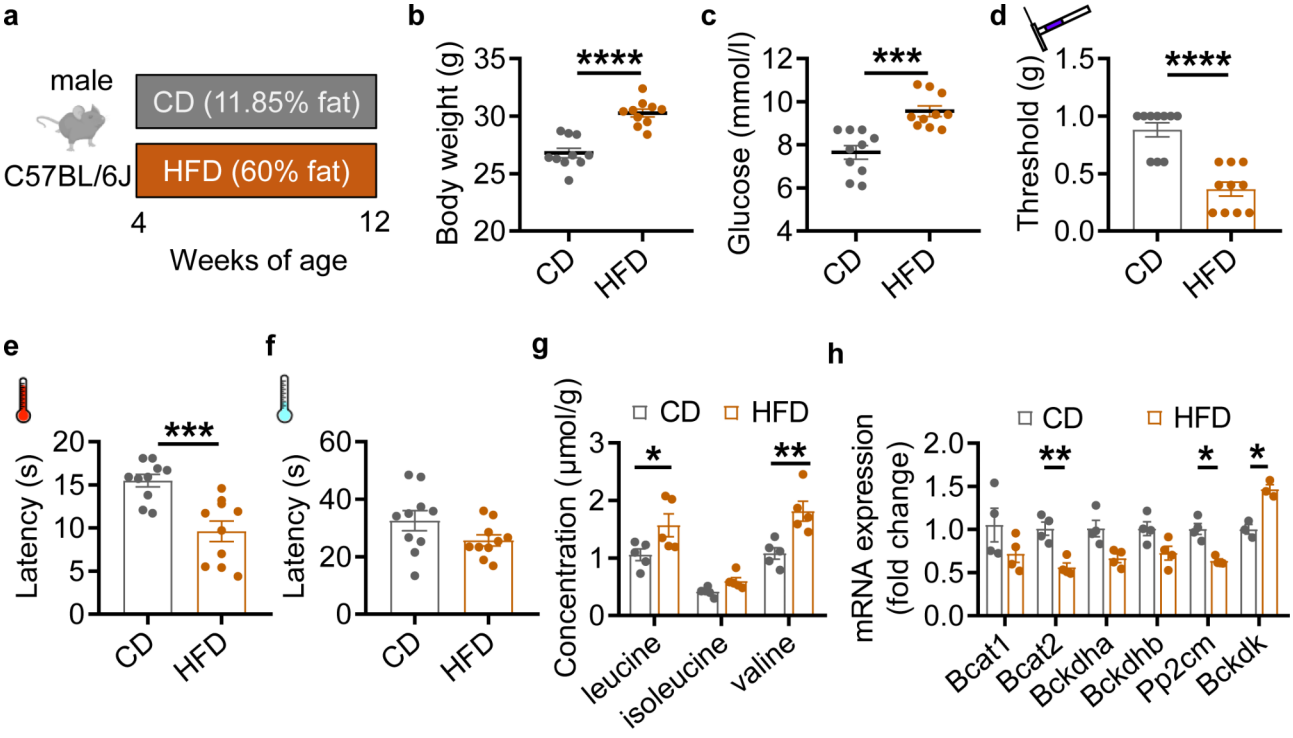

Fig. 1 Impaired BCAA catabolism in lumbar 4–5 DRG of 8-week HFD mice

a, Schematic of high-fat diet (HFD) model, showing male 4-week-old C57BL/6J mice were fed with either standard chow diet (CD) or HFD for 8 weeks. **b**, **c**, Body weight (**b**) and nonfasting blood glucose levels (**c**) were measured after 8 weeks of CD or HFD feeding. $n=10$ mice/group. **d-f**, Mechanical withdrawal thresholds (**d**), withdrawal latencies to heat (**e**), and cold stimulus (**f**) were measured after 8 weeks of feeding with CD or HFD. $n=10$ mice/group. **g**, BCAA concentrations in the lumbar 4–5 (L4-L5) DRGs of mice after an 8-week feeding of CD or HFD. $n=5$ mice/group. **h**, Relative mRNA expression of BCAA catabolic enzymes, *Bcat1*, *Bcat2*, *Bckdha*, *Bckdhb*, *Pp2cm*, and *Bckdk* (to *β-actin*) in the L4-L5 DRGs after 8 weeks of CD or HFD feeding. $n=3$–4 experimental repeats (8 mice)/group. Data are shown as the mean ± SEM. Statistical tests used were unpaired two-tailed Student's *t*-test (**b-f**), and two-way repeated-measures ANOVA with Bonferroni's post hoc test (**g**, **h**). *$p<0.05$, **$p<0.01$, ***$p<0.005$, and ****$p<0.001$

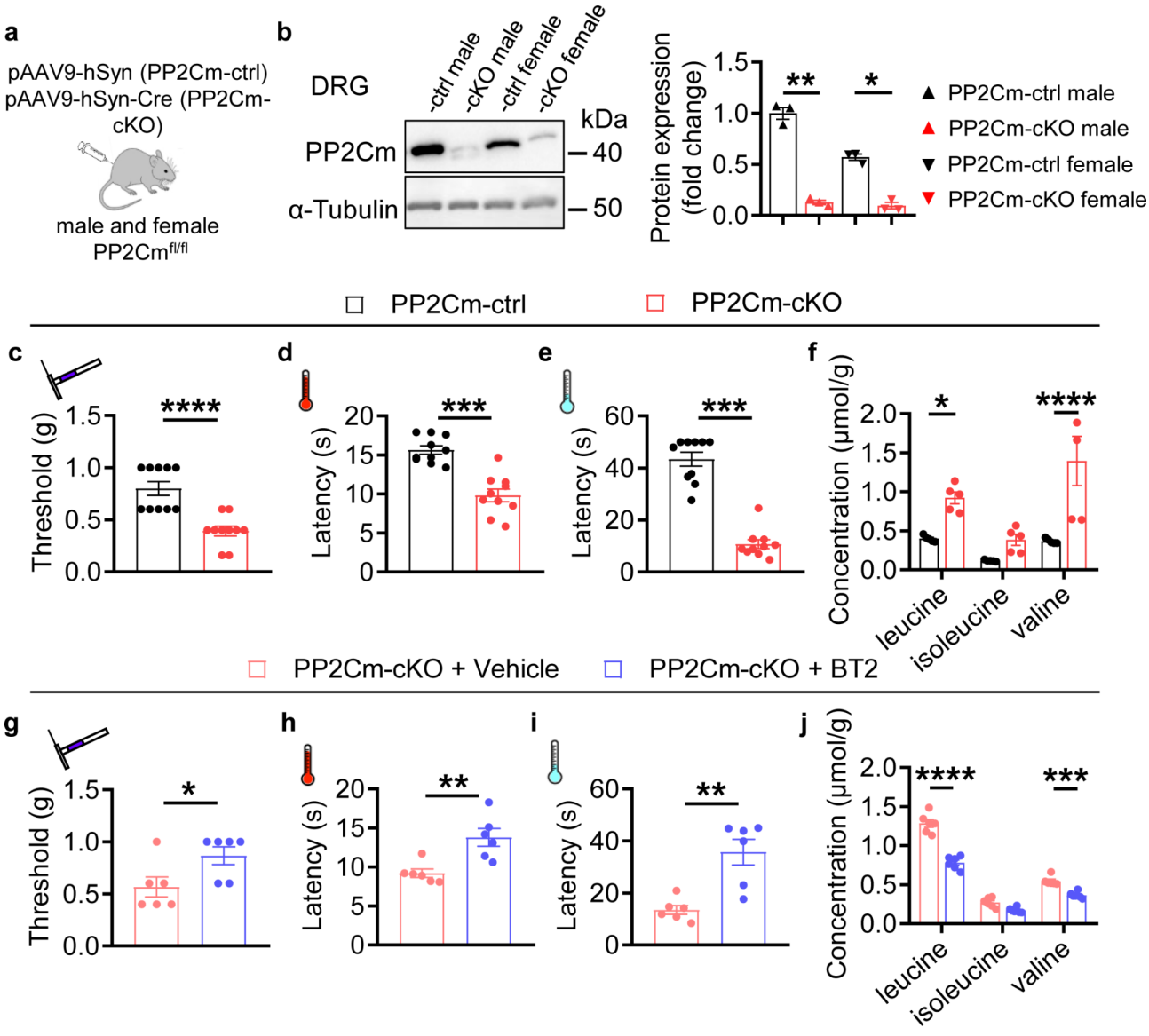

Fig. 2 Conditional knockout of PP2Cm in DRG neurons induces pain hypersensitivity

a, Representative cartoons of pAAV9-hSyn-(Cre) injection. Intrathecal injection of pAAV9-hSyn-Cre or pAAV9-hSyn into male and female PP2Cm$^{fl/fl}$ mice resulted in the generation of PP2Cm-cKO and PP2Cm-ctrl mice. **b**, Representative immunoblots of PP2Cm in the L4-L5 DRGs on day 21 post-injection in PP2Cm-cKO and PP2Cm-ctrl mice of both sexes. male $n=3$ experimental repeats (6 mice)/group, female $n=3$ experimental repeats (6 mice)/group. **c-e**, Mechanical withdrawal thresholds (**c**), withdrawal latencies to heat (**d**) and cold stimulus (**e**) in PP2Cm-cKO and PP2Cm-ctrl mice. $n=10$ mice/group, both sexes. **f**, BCAA concentrations in the L4-L5 DRGs of PP2Cm-cKO and PP2Cm-ctrl mice. $n=5$ mice/group, both sexes. **g-i**, Mechanical withdrawal thresholds (**g**), withdrawal latencies to heat (**h**) and cold stimulus (**i**) in PP2Cm-cKO mice with or without BT2 supplementation after 7 consecutive days, PP2Cm-cKO + Vehicle vs. PP2Cm-cKO + BT2. $n=6$ mice/group, both sexes. **j**, BCAA concentrations in the L4-L5 DRGs of PP2Cm-cKO + Vehicle and PP2Cm-cKO + BT2 mice. $n=6$ mice/group, both sexes. Data are shown as the mean ± SEM. Statistical tests used were unpaired two-tailed Student's *t*-test (**c-e**, **g-i**), one-way ANOVA with Tukey's multiple comparisons test (**b**), and two-way repeated-measures ANOVA with Bonferroni's post hoc test (**f**, **j**). *$p<0.05$, **$p<0.01$, ***$p<0.005$, and ****$p<0.001$

both sexes (Fig. 2b; male $p=0.006$, female $p=0.01$). This reduction was not observed in the L4-L5 dorsal spinal cord (DSC), heart, brain, liver, muscle or adipose tissue (Fig. S2a). Body weight and nonfasting blood glucose levels in PP2Cm-cKO mice were comparable to these in PP2Cm-ctrl mice, irrespective of sex (Fig. S2b, c). Behavioral assessments showed that PP2Cm-cKO mice of both sexes exhibited mechanical allodynia, and heat and cold hyperalgesia on 21 d post-injection (Fig. 2c-e, mechanical thresholds $p<0.0001$, heat latencies $p<0.001$, cold latencies $p<0.001$; Fig. S2d-f). Because no difference was observed in pain phenotype between male and female PP2Cm-cKO mice, subsequent experimental results were obtained from mice of both sexes. Additionally, BCAA

concentrations in the L4-L5 DRGs of PP2Cm-cKO mice were significantly elevated (Fig. 2f; leucine $p=0.04$, isoleucine $p=0.44$, valine $p<0.0001$).

To further determine whether BCAA accumulation in PP2Cm-cKO mice was responsible for pain hypersensitivity, we promoted BCAA catabolism via daily gavage of BT2, an activator of BCKDH, for 7 consecutive days. Systemic BT2 treatment substantially prevented the decreases in nociceptive thresholds to mechanical, heat, and cold stimulation, and markedly eliminated BCAA concentrations in the L4-L5 DRGs (Fig. 2g-j; mechanical thresholds $p=0.04$, heat latencies $p=0.004$, cold latencies $p=0.002$; leucine $p<0.0001$, isoleucine $p=0.07$, valine $p=0.0006$). These results indicate that defective BCAA catabolism in the DRG contributes to pain hypersensitivity.

BCAA catabolic defects in DRG neurons activate the CCL5/CCR5 axis

To better understand how BCAA catabolic defects induce pain sensitization, we performed RNA sequencing of the L4-L5 DRGs of PP2Cm-ctrl and PP2Cm-cKO mice. Transcriptional landscape analysis identified 498 upregulated genes and 37 downregulated genes in PP2Cm-cKO mice compared to -ctrl mice (Fig. 3a, Fig. S3a). By KEGG pathway analysis, multiple proinflammatory pathways, including the B-cell receptor, extracellular matrix (ECM) receptor interaction, cytokine-cytokine receptor interaction, P53 and chemokine signaling were recognized as the significantly and heavily enriched pathways in PP2Cm-cKO mice (Fig. 3b, Supplementary Table S2). In this study, we compared the FPKM values of a large scope of chemokines, which contribute to the pathogenesis of pain. *Ccl5* was predicted to be the most significantly altered gene in PP2Cm-cKO mice (Fig. S3b). Subsequently, qPCR confirmed a ~ 65-fold increase in *Ccl5* and a ~ 3.2-fold increase in *Ccr5* mRNA expression in the L4-L5 DRGs of PP2Cm-cKO mice (Fig. 3c, d; *Ccl5* $p<0.001$, *Ccr5* $p<0.001$). The expression of proinflammatory cytokines, such as *Tnf-α* and *Il-1β*, were also upregulated (Fig. 3e, f; *Tnf-α* $p=0.05$, *Il-1β* $p=0.001$). An 8-week HFD also increased the mRNA levels of *Ccl5*, *Ccr5*, *Tnf-α*, and *Il-1β* in the L4-L5 DRGs (Fig. S3c-f; *Ccl5* $p<0.0001$, *Ccr5* $p=0.03$, *Tnf-α* $p<0.0001$, *Il-1β* $p=0.01$). To further determine if promoting BCAA catabolism could suppress DRG inflammation, BT2 was administered to PP2Cm-cKO and HFD-fed mice, respectively. Notably, BT2 significantly reversed the upregulation of *Ccl5*, *Ccr5*, *Tnf-α* and/or *Il-1β* in the L4-L5 DRGs of PP2Cm-cKO and HFD-fed mice (Fig. 3g-j, *Ccl5* $p=0.04$, *Ccr5* $p=0.01$, *Tnf-α* $p=0.03$, *Il-1β* $p=0.03$; Fig. S3g-j, *Ccl5* $p=0.03$, *Ccr5* $p=0.03$, *Tnf-α* $p=0.03$, *Il-1β* $p=0.04$). These results indicate that PP2Cm deletion leads to the activation of CCL5/CCR5 axis and a proinflammatory status in the DRG.

Targeting the CCL5/CCR5 axis alleviates pain behaviors in DRG specific PP2Cm-knockout mice

Elevated CCL5 levels in the L4-L5 DRGs of PP2Cm-cKO mice were confirmed by ELISA kits (Fig. 4a; $p<0.001$). To determine if elevated CCL5 was involved in the development of pain hypersensitivity, PP2Cm-cKO mice were intrathecally administered an anti-CCL5 neutralizing antibody for 2 consecutive days (Fig. 4b). One day after injection with the anti-CCL5 antibody, PP2Cm-cKO mice exhibited decreased CCL5 levels, along with ameliorative mechanical allodynia and cold hyperalgesia, without an effect on heat hyperalgesia. However, at 3 d, these mice had recovered to a hypersensitive state with restored CCL5 levels in the L4-L5 DRGs (Fig. 4c-f).

The amount of CCR5 protein was elevated by 1.2-fold in the L4-L5 DRGs of PP2Cm-cKO mice, as compared to the PP2Cm-ctrl mice (Fig. S4a; $p=0.005$). We further detected the expression of CCR5 in DRG neurons using immunohistochemistry. CCR5 expression was markedly upregulated in PP2Cm-cKO mice (Fig. 4g-i). To investigate the role of CCR5 in PP2Cm-cKO mice, we inhibited CCR5 increase via intrathecal injection of maraviroc, a specific antagonist, or *Ccr5*-directed small interfering RNA (siCcr5) (Fig. 4j). Maraviroc alleviated mechanical allodynia and thermal (heat and cold) hyperalgesia in PP2Cm-cKO mice within 1 h post-injection, but the analgesic effect disappeared 24 h later (Fig. 4k-m). Intrathecal administration of siCcr5 significantly decreased *Ccr5* mRNA levels in the L4-L5 DRGs and ameliorated mechanical allodynia and thermal hyperalgesia in PP2Cm-cKO mice on day 2 post-injection. However, *Ccr5* expression and nociceptive hypersensitivity in these mice had returned to baseline levels on day 8 post-injection (Fig. 4n-q). Furthermore, we measured chemokine and cytokine mRNA levels after siCcr5 treatment in PP2Cm-cKO mice. Consequently, *Ccr5* knockdown reduced the mRNA levels of *Ccl5*, *Tnf-α* and *Il-1β* in the L4-L5 DRGs (Fig. S4b-d). Therefore, our data indicate that pharmacological inhibition or genetic knockdown of the CCL5/CCR5 pathway can mitigate hyperalgesia in PP2Cm-cKO mice accompanied by decreased expression of chemokines and cytokines.

Upregulated TRPA1 expression mediates pain hypersensitivity in DRG specific PP2Cm-knockout mice

Inflammatory signals alter the expression of TRPA1 and TRPV1, contributing to hyperalgesia [6]. We investigated whether the expression of TRPA1 and TRPV1 were upregulated in PP2Cm-cKO mice. Quantitative PCR revealed that the mRNA level of *Trpa1*, but not *Trpv1*, was increased by 1.9-fold in the L4-L5 DRGs

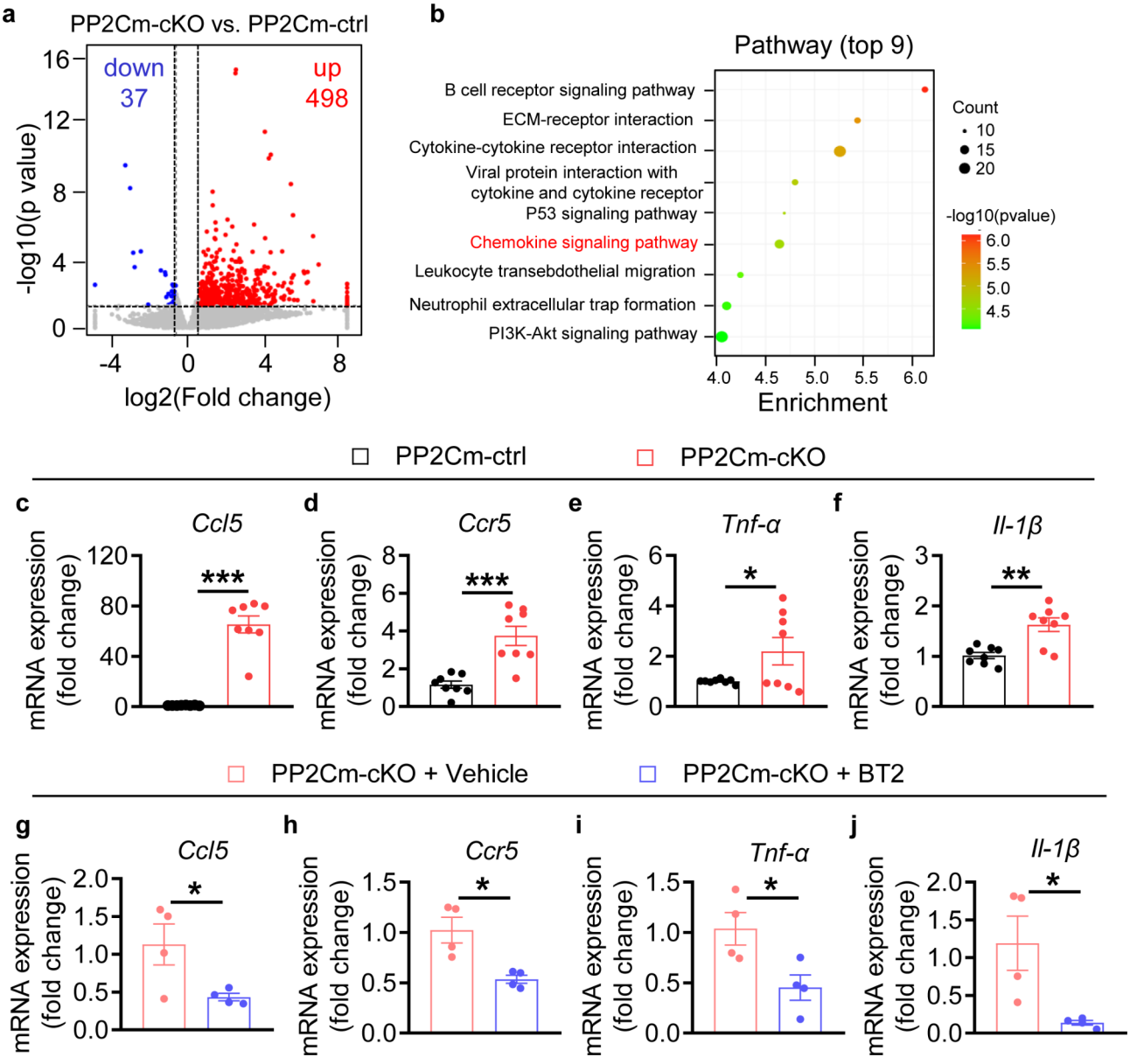

Fig. 3 The neuron-specific deletion of PP2Cm in DRG induces the upregulation of CCL5/CCR5 pathway and other proinflammatory cytokines **a**, Volcano plot illustrated the transcriptomics analysis of the L4-L5 DRGs from PP2Cm-cKO and PP2Cm-ctrl mice. Significantly upregulated genes are colored in red, downregulated genes are in blue, and unchanged genes are in grey. $n = 3$ experimental repeats (9 mice)/group. **b**, Top 9 significantly enriched pathways identified in KEGG enrichment analysis of L4-L5 DRGs from PP2Cm-cKO and PP2Cm-ctrl mice. **c-f**, The mRNA levels of *Ccl5* (**c**), *Ccr5* (**d**), *Tnf-α* (**e**), and *Il-1β* (**f**) in the L4-L5 DRGs of PP2Cm-ctrl and PP2Cm-cKO mice (to *β-actin*). $n = 8$ experimental repeats (16 mice)/group. **g-j**, The mRNA levels of *Ccl5* (**g**), *Ccr5* (**h**), *Tnf-α* (**i**), and *Il-1β* (**j**) in the L4-L5 DRGs of PP2Cm-cKO + Vehicle and PP2Cm-cKO + BT2 (to *β-actin*). $n = 4$ experimental repeats (8 mice)/group. Data are shown as the mean ± SEM. Statistical tests used were unpaired two-tailed Student's t-test (**c-j**). $^{*}p < 0.05$, $^{**}p < 0.01$, and $^{***}p < 0.005$

of PP2Cm-cKO mice (Fig. 5a, *Trpa1* $p=0.03$; Fig. S5a, *Trpv1* $p=0.43$). TRPA1 protein expression was also elevated by 1.3-fold in the L4-L5 DRGs of PP2Cm-cKO mice, as compared to those in PP2Cm-ctrl mice (Fig. 5b, $p=0.04$). We further characterized TRPA1 expression in sensory neurons. In the L4-L5 DRGs of PP2Cm-cKO and PP2Cm-ctrl mice, TRPA1 was most likely expressed in CGRP-positive neurons, as well as in IB_4-positive neurons (Fig. 5c, d), but was absent in NF200-positive neurons (Fig. S5b). Importantly, systemic BT2 treatment reversed the upregulation of *Trpa1* mRNA in the L4-L5 DRGs of PP2Cm-cKO mice (Fig. 5e; $p<0.001$). Intrathecal siCcr5 administration also reduced *Trpa1* mRNA level in the L4-L5 DRGs of PP2Cm-cKO mice on day 2 post-injection (Fig. 5f). Additionally, in 8-week HFD-fed mice, the *Trpa1* mRNA level was increased by 1.7-fold, and this upregulation was blunted by systemic BT2 administration (Fig. S5c, d).

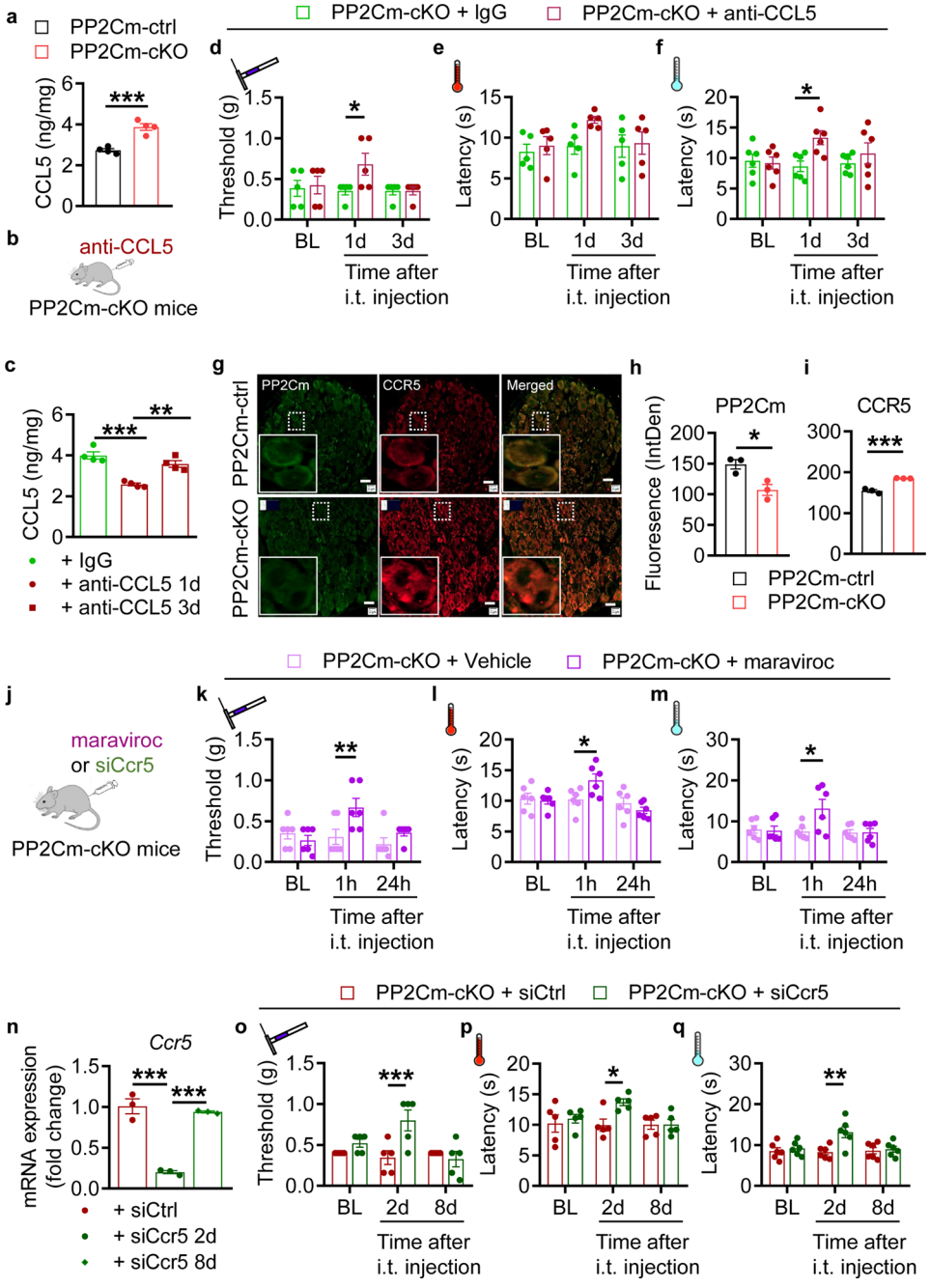

Fig. 4 Inhibiting the CCL5/CCR5 signaling pathway attenuates hyperalgesia in DRG PP2Cm-deficient mice

a, Quantification for release of CCL5 in the L4-L5 DRGs of PP2Cm-ctrl and PP2Cm-cKO mice, as detected by ELISA. $n = 4$ mice/group. **b**, Illustrative cartoon depicting the intrathecal administration of an anti-CCL5 neutralizing antibody. **c**, Quantification for release of CCL5 in the L4-L5 DRGs of PP2Cm-cKO + IgG, PP2Cm-cKO + anti-CCL5 1d and PP2Cm-cKO + anti-CCL5 3d mice. $n = 4$ mice/group. **d-f**, Mechanical withdrawal thresholds (**d**), withdrawal latencies to heat (**e**) and cold stimulus (**f**) on day 0 (baseline, BL), 1, and 3 post-injection in PP2Cm-cKO mice treated with IgG or anti-CCL5 neutralizing antibody. $n = 5$–6 mice/group. **g**, The L4-L5 DRGs from PP2Cm-ctrl and PP2Cm-cKO mice were double stained with PP2Cm (green) and CCR5 (red). The corner image in white square is the zoomed-in image of the area in the smaller white square. Scale bar: 20 μm. **h**, **i**, Fluorescent quantifications for PP2Cm (**h**) and CCR5 (**i**) in DRG sections from PP2Cm-ctrl and PP2Cm-cKO mice. $n = 3$ sections from 3 mice/group. **j**, A representative cartoon illustrating the intrathecal injection of CCR5 antagonist maraviroc or *Ccr5* small interfering RNA (siCcr5). **k-m**, Mechanical withdrawal thresholds (**k**), withdrawal latencies to heat (**l**) and cold stimulus (**m**) at BL, 1 h, and 24 h post-injection in PP2Cm-cKO mice treated with Vehicle or maraviroc. $n = 6$ mice/group. **n**, The mRNA levels of *Ccr5* in the L4-L5 DRGs from PP2Cm-cKO + siCtrl, PP2Cm-cKO + siCcr5 2d, and PP2Cm-cKO + siCcr5 8d mice (to *β-actin*). $n = 3$ experimental repeats (6 mice)/group. **o-q**, Mechanical withdrawal thresholds (**o**), withdrawal latencies to heat (**p**) and cold stimulus (**q**) at BL, 2d, and 8d post-injection in PP2Cm-cKO mice treated with siCtrl or siCcr5. $n = 5$–6 mice/group. Data are shown as the mean ± SEM. Statistical tests used were unpaired two-tailed Student's *t*-test (**a**, **h**, **i**), one-way ANOVA with Tukey's multiple comparisons test (**c**, **n**), and two-way repeated-measures ANOVA with Bonferroni's post hoc test (**d-f**, **k-m**, **o-q**). $^{*}p < 0.05$, $^{**}p < 0.01$, and $^{***}p < 0.005$

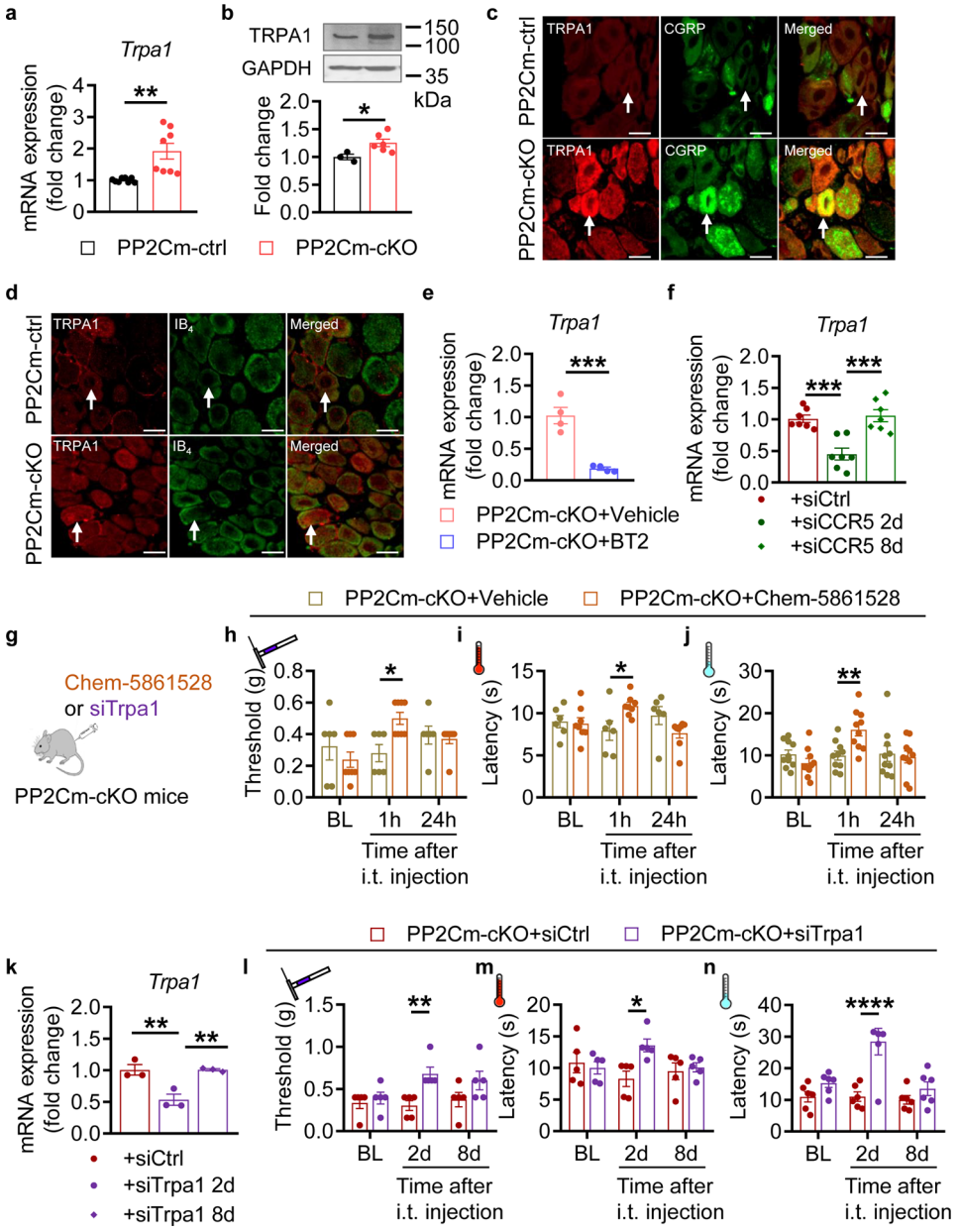

Fig. 5 Increased TRPA1 expression mediates pain hypersensitivity in DRG specific PP2Cm-knockout mice

a, The *Trpa1* mRNA level in the L4-L5 DRGs of PP2Cm-ctrl and PP2Cm-cKO mice (to *β-actin*). $n = 8$ experimental repeats (16 mice)/group. **b**, Representative immunoblots and protein levels of TRPA1 in the L4-L5 DRGs from PP2Cm-cKO and PP2Cm-ctrl mice (to GAPDH). $n = 3$–6 experimental repeats (6–12 mice)/group. **c**, **d**, Double-labelled immunofluorescent staining of TRPA1 (red) with calcitonin gene-related peptide (CGPR, green, **c**) or isolectin B_4 (IB_4; green, **d**) in the L4-L5 DRGs from PP2Cm-ctrl and PP2Cm-cKO mice. White arrowheads indicate double positive neurons. $n = 4$–5 sections from 5 mice/group. Scale bar: 20 μm. **e**, The *Trpa1* mRNA level in the L4-L5 DRGs of PP2Cm-cKO + Vehicle and PP2Cm-cKO + BT2 mice (to *β-actin*). $n = 4$ experimental repeats (8 mice)/group. **f**, The *Trpa1* mRNA level in the L4-L5 DRGs of PP2Cm-cKO + siCtrl, PP2Cm-cKO + siCcr5 2d, and PP2Cm-cKO + siCcr5 8d mice (to *β-actin*). $n = 7$ experimental repeats (14 mice)/group. **g**, A representative cartoon illustrating the intrathecal injection of TRPA1 inhibitor chem-5,861,528 or *Trpa1* small interfering RNA (siTrpa1). **h-j**, Mechanical withdrawal thresholds (**h**), withdrawal latencies to heat (**i**) and cold stimuli (**j**) at baseline (BL), 1 h, and 24 h post-injection in PP2Cm-cKO mice treated with Vehicle or chem-5,861,528. $n = 6$–10 mice/group. **k**, The *Trpa1* mRNA level in the L4-L5 DRGs of PP2Cm-cKO + siCtrl, PP2Cm-cKO + siTrpa1 2 d and PP2Cm-cKO + siTrpa1 8 d mice (to *β-actin*). $n = 3$ experimental repeats (6 mice)/group. **l-n**, Mechanical withdrawal thresholds (**l**), withdrawal latencies to heat (**m**) and cold stimuli (**n**) at BL, 2d, and 8d post-injection in PP2Cm-cKO mice treated with siCtrl or siTrpa1. $n = 5$–6 mice/group. Data are shown as the mean ± SEM. Statistical tests used were unpaired two-tailed Student's *t*-test (**a**, **b**, **e**), one-way ANOVA with Tukey's multiple comparisons test (**f**, **k**), and two-way repeated-measures ANOVA with Bonferroni's post hoc test (**h-j**, **l-n**). $^{*}p < 0.05$, $^{**}p < 0.01$, $^{***}p < 0.005$, and $^{****}p < 0.001$

Finally, in order to determine whether upregulated TRPA1 in DRG contributed to pain hypersensitivity in PP2Cm-cKO mice, we intrathecally administered Chem-5,861,528, a specific TRPA1 inhibitor, or *Trpa1*-targeting siRNA (siTrpa1) to these mice (Fig. 5g). Chem-5,861,528 effectively attenuated mechanical allodynia, heat, and cold hyperalgesia within 1 h post-injection in PP2Cm-cKO mice, but these antinociceptive effects disappeared 24 h after administration (Fig. 5h-j). The siTrpa1, but not siCtrl, effectively blocked PP2Cm-cKO-induced increase in *Trpa1* mRNA level in the L4-L5 DRGs, and mitigated the PP2Cm-cKO-induced mechanical, heat, and cold hyperalgesia on day 2 post-injection (Fig. 5k-n). In addition, siTrpa1 treatment substantially inhibited the *Tnf-α* and *Il-1β* mRNA expression (Fig. S5e, f). Together, the above results indicate that the upregulated TRPA1 expression in DRG mediates PP2Cm deletion-induced pain hypersensitivity.

Discussion

Our previous studies have shown a correlation between BCAA accumulation and pain hypersensitivity, but the exact mechanism remains elusive [15]. In the present study, we demonstrated that high-fat diet induced nociceptive hypersensitivity in male mice, and BCAA catabolism was impaired in their L4-L5 DRGs. Additionally, conditional deletion of PP2Cm in DRG neurons led to mechanical allodynia, heat and cold hyperalgesia in both sexes. Mechanistically, genetic knockout of PP2Cm resulted in the upregulation of CCL5/CCR5 axis and a proinflammatory status in the L4-L5 DRGs, and increased TRPA1 expression. Pharmacological inhibition and genetic intervention of the CCL5/CCR5 axis or TRPA1 can attenuate pain behaviors induced by PP2Cm knockout. Therefore, our results reveal a novel mechanism by which BCAA catabolism in the L4-L5 DRGs regulates pain behaviors.

The current understanding of the relationship between BCAA metabolism and aberrant nociception is very limited. We first identified that 8-week HFD induced nociceptive hypersensitivity and impaired BCAA catabolism in the L4-L5 DRGs. Subsequently, we extended our research to investigate the hypothesis that BCAA metabolic dysfunction in DRG contributes to pain hypersensitivity. The conditional deletion of PP2Cm in DRG neurons increased nociceptive responses to mechanical and thermal (heat and cold) stimuli, and these hypersensitivities could be mitigated by promoting BCAA catabolism via BT2 treatment. The AAV9 vector is characterized by its efficient transduction of DRG neurons following intrathecal delivery [39]. In this study, intrathecal delivery of pAAV9-hSyn-Cre preferentially deleted PP2Cm in the L4-L5 DRGs rather than the dorsal spinal cord. This preference may be attributed to the following two factors: (1) limited transduction efficiency of spinal cord dorsal horn neurons via intrathecal delivery [31, 32]; (2) the hSyn promoter's inability to drive expression in a subset of dorsal horn neurons, despite its pan-neuronal profile [24].

Elevated BCAAs activate inflammatory pathways and increase the release of proinflammatory mediators [23, 46]. Transcriptional profiling revealed a proinflammatory state in the L4-L5 DRGs of PP2Cm-cKO mice, with *Ccl5* mRNA being the most significantly upregulated chemokine. Then, we found that the mRNA levels of *Ccl5*, *Ccr5*, *Tnf-α*, and *Il-1β* were increased in the L4-L5 DRGs of PP2Cm-cKO and HFD-fed mice. Enhancing BCAA catabolism with systemic BT2 treatment markedly reduced the expression of these genes, supporting the notion that BT2 can be a promising anti-inflammatory agent for clinical pain management [41]. Proinflammatory mediators sensitize afferent neurons and consequently lead to hyperalgesia [38]. CCL5 is recognized as a potential target for modulating the migration of inflammatory cells and controlling hyperalgesia at peripheral injured sites in chronic pain models [16, 19]. CCR5, which is expressed in sensory neurons, acts as a pathological regulator in the pathogenesis of pain and directly enhances pain sensitivity [21, 26]. In this study, we intrathecally administered anti-CCL5 neutralizing antibody, maraviroc, or *Ccr5*-directed small interfering RNA to PP2Cm-cKO mice, which could alleviate nociceptive hypersensitivity. Thus, our results suggest that the CCL5/CCR5 axis in DRG is involved in the genesis of pain hypersensitivity induced by PP2Cm knockout.

CCL5-induced hyperalgesia is associated with TRPA1 sensitization [6]. Inflammation induces TRPA1 trafficking to cell membrane and increases its membrane expression [18, 36, 42]. The findings comparing TRPA1 expression in obese and lean mice are seemingly paradoxical: some studies reporting increased expression in obese mice [33], while others reporting no alteration [29]. In this study, we found that *Trpa1* expression was increased in the L4-L5 DRGs of HFD-fed mice. In PP2Cm-cKO mice, TRPA1 protein expression was also elevated and present in CGRP- and IB_4-positive neurons [8]. TRPA1 channel is involved in the maintenance of pain hypersensitivity [9, 22]. Studies have demonstrated that systemic administration of Chem-5,861,528, a selective TRPA1 channel antagonist, or TRPA1 gene deletion, can attenuate nociceptive hypersensitivity in pain models [9, 10, 35]. In this study, intrathecal administration of Chem-5,861,528 produced anti-nociceptive effects, and knockdown of TRPA1 in the L4-L5 DRGs also alleviated nociceptive hypersensitivity in PP2Cm-cKO mice.

Our study builds upon previous findings and extends to investigate the role for BCAA catabolism in regulating pain behaviors. Further work is needed to address

the limitations of the present study. First, we used small interfering RNA to silence the expression of CCR5 and TRPA1 genes; however, siRNA may have potential off-target effects and lack the cell type transfection selectivity, thus additional PP2Cm-CCR5 and PP2Cm-TRPA1 double knockout mice are required to ascertain the role of these genes in pain hypersensitivity. Furthermore, the results indicated that upregulated TRPA1 expression in the DRG mediated PP2Cm deletion-induced pain hypersensitivity, and more electrophysiology studies are needed to measure TRPA1 currents. Future research incorporating electrophysiology can better elucidate the roles of ion channels in pain sensitization induced by DRG-specific PP2Cm knockout.

Conclusions

We identified that conditional deletion of PP2Cm in DRG neurons led to mechanical allodynia, heat and cold hyperalgesia. Genetic PP2Cm knockout activated the CCL5/CCR5 axis and upregulated TRPA1 expression. Inhibiting elevated CCL5/CCR5 axis or TRPA1 can attenuate pain behaviors induced by PP2Cm knockout. The present study unveils a critical role of BCAA catabolism in pain sensitization, which may serve as a basis for pain pathogenesis, as well as a potential target for pain therapy.

Abbreviations

DRG	dorsal root ganglion
BCAA	branched-chain amino acid
CD	chow diet
HFD	high-fat diet
PP2Cm	mitochondrial targeted 2 C-type serine/threonine protein phosphatase
BCAT1	branched-chain amino-transferase 1
BCAT2	branched-chain amino-transferase 2
BCKDHA	branched-chain alpha-ketoacid dehydrogenase A
BCKDHB	branched-chain alpha-ketoacid dehydrogenase B
BCKDK	branched-chain ketoacid dehydrogenase kinase
cKO	conditional knockout
DSC	dorsal spinal cord
CCL5	C-C chemokine ligand 5
CCR5	C-C chemokine receptor 5
TRPA1	transient receptor potential ankyrin 1
TNF-α	tumor necrosis factor α
IL-1β	interleukin-1β

Supplementary Information

The online version contains supplementary material available at https://doi.org/10.1186/s40478-024-01856-2.

Supplementary Material 1

Acknowledgements

We thank American Journal Experts (AJE) for their professional English language editing services.

Author contributions

NL and PL designed the study. NL and FL performed the animal models, pain behavioral studies, western blotting, quantitative real-time PCR, and RNA sequencing. YY performed ELISA and immunohistochemistry. YK performed the measurement of BCAA concentrations. KL performed intrathecal injection. SL and TL performed the data analysis. PL and CZ wrote the manuscript. All authors read and approved the final version.

Funding

This study was supported in part by grants from the STI2030-Major Projects (Project No. 2021ZD0201904), the National Key R&D Program of China (Project Nos. 2022YFC2009901 and 2022YFC2009900), the National Natural Science Foundation of China (Project No. 81801117), and the Sichuan Science and Technology Program (Project Nos. 2023ZYD0168, 2023NSFSC1734, and 2024NSFSC0616).

Data availability

The datasets used and/or analyzed during the current study available from the corresponding author on reasonable request.

Declarations

Ethics approval

All procedures were approved by the Animal Ethics Committee of West China Hospital, Sichuan University, China (Protocol No.20230310052).

Consent for publication

Not applicable.

Competing interests

The authors declare that they have no competing interests.

Received: 18 July 2024 / Accepted: 31 August 2024
Published online: 10 September 2024

References

1. Basbaum AI, Bautista DM, Scherrer G, Julius D (2009) Cellular and molecular mechanisms of pain. Cell 139:267–284
2. Boyd JT, LoCoco PM, Furr AR, Bendele MR, Tram M, Li Q et al (2021) Elevated dietary ω-6 polyunsaturated fatty acids induce reversible peripheral nerve dysfunction that exacerbates comorbid pain conditions. Nat Metab 3:762–773
3. Escolano-Lozano F, Buehling-Schindowski F, Kramer HH, Birklein F, Geber C (2022) Painful Diabetic Neuropathy: Myofascial Pain makes the difference. Diabetes Care 45:e139–e140
4. Feldman EL, Callaghan BC, Pop-Busui R, Zochodne DW, Wright DE, Bennett DL et al (2019) Diabetic neuropathy. Nat Rev Dis Primers 5:42
5. Gangadharan V, Kuner R (2013) Pain hypersensitivity mechanisms at a glance. Dis Model Mech 6:889–895
6. González-Rodríguez S, Álvarez MG, García-Domínguez M, Lastra A, Cernuda-Cernuda R, Folgueras AR et al (2017) Hyperalgesic and hypoalgesic mechanisms evoked by the acute administration of CCL5 in mice. Brain Behav Immun 62:151–161
7. Haque MM, Kuppusamy P, Melemedjian OK (2024) Disruption of mitochondrial pyruvate oxidation in dorsal root ganglia drives persistent nociceptive sensitization and causes pervasive transcriptomic alterations. Pain 165:1531–1549
8. Hiyama H, Yano Y, So K, Imai S, Nagayasu K, Shirakawa H et al (2018) TRPA1 sensitization during diabetic vascular impairment contributes to cold hypersensitivity in a mouse model of painful diabetic peripheral neuropathy. Mol Pain 14:174480691878981
9. Koivisto A, Pertovaara A (2013) Transient receptor potential ankyrin 1 (TRPA1) ion channel in the pathophysiology of peripheral diabetic neuropathy. Scand J Pain 4:129–136
10. Koivisto A, Hukkanen M, Saarnilehto M, Chapman H, Kuokkanen K, Wei H et al (2012) Inhibiting TRPA1 ion channel reduces loss of cutaneous nerve fiber function in diabetic animals: sustained activation of the TRPA1 channel contributes to the pathogenesis of peripheral diabetic neuropathy. Pharmacol Res 65:149–158
11. Kwiatkowski K, Piotrowska A, Rojewska E, Makuch W, Jurga A, Slusarczyk J et al (2016) Beneficial properties of maraviroc on neuropathic pain development and opioid effectiveness in rats. Prog Neuropsychopharmacol Biol Psychiatry 64:68–78

12. Kwiatkowski K, Ciapala K, Rojewska E, Makuch W, Mika J (2020) Comparison of the beneficial effects of RS504393, maraviroc and cenicriviroc on neuropathic pain-related symptoms in rodents: behavioral and biochemical analyses. Int Immunopharmacol 84:106540
13. Li T, Zhao L, Li Y, Dang M, Lu J, Lu Z et al (2023) PPM1K mediates metabolic disorder of branched-chain amino acid and regulates cerebral ischemia-reperfusion injury by activating ferroptosis in neurons. Cell Death Dis 14:634
14. Lian K, Guo X, Wang Q, Liu Y, Wang RT, Gao C et al (2020) PP2Cm overexpression alleviates MI/R injury mediated by a BCAA catabolism defect and oxidative stress in diabetic mice. Eur J Pharmacol 866:172796
15. Lian N, Luo KT, Xie HJ, Kang Y, Tang K, Lu PL et al (2022) Obesity by High-Fat Diet increases Pain Sensitivity by Reprogramming branched-chain amino acid catabolism in dorsal Root Ganglia. Front Nutr 9:902635
16. Liou JT, Yuan HB, Mao CC, Lai YS, Day YJ (2012) Absence of C-C motif chemokine ligand 5 in mice leads to decreased local macrophage recruitment and behavioral hypersensitivity in a murine neuropathic pain model. Pain 153:1283–1291
17. Liou JT, Mao CC, Ching-Wah Sum D, Liu FC, Lai YS, Li JC et al (2013) Peritoneal administration of Met-RANTES attenuates inflammatory and nociceptive responses in a murine neuropathic pain model. J Pain 14:24–35
18. Mahajan N, Khare P, Kondepudi KK, Bishnoi M (2021) TRPA1: Pharmacology, natural activators and role in obesity prevention. Eur J Pharmacol 912:174553
19. Malon JT, Cao L (2016) Calcitonin gene-related peptide contributes to peripheral nerve injury-induced mechanical hypersensitivity through CCL5 and p38 pathways. J Neuroimmunol 297:68–75
20. Marques RE, Guabiraba R, Russo RC, Teixeira MM (2013) Targeting CCL5 in inflammation. Expert Opin Ther Targets 17:1439–1460
21. Matsushita K, Tozaki-Saitoh H, Kojima C, Masuda T, Tsuda M, Inoue K et al (2014) Chemokine (C-C motif) receptor 5 is an important pathological regulator in the development and maintenance of neuropathic pain. Anesthesiology 120:1491–1503
22. Meents JE, Ciotu CI, Fischer MJM (2019) TRPA1: a molecular view. J Neurophysiol 121:427–443
23. Papathanassiu AE, Ko JH, Imprialou M, Bagnati M, Srivastava PK, Vu HA et al (2017) BCAT1 controls metabolic reprogramming in activated human macrophages and is associated with inflammatory diseases. Nat Commun 8:16040
24. Peirs C, Williams S-PG, Zhao X, Arokiaraj CM, Ferreira DW, Noh M-c et al (2021) Mechanical Allodynia Circuitry in the dorsal horn is defined by the nature of the Injury. Neuron 109:73–90e77
25. Rojas DR, Kuner R, Agarwal N (2019) Metabolomic signature of type 1 diabetes-induced sensory loss and nerve damage in diabetic neuropathy. J Mol Med (Berl) 97:845–854
26. Shen Y, Zhou M, Cai D, Filho DA, Fernandes G, Cai Y et al (2022) CCR5 closes the temporal window for memory linking. Nature 606:146–152
27. Singh OV, Yaster M, Xu JT, Guan Y, Guan X, Dharmarajan AM et al (2009) Proteome of synaptosome-associated proteins in spinal cord dorsal horn after peripheral nerve injury. Proteomics 9:1241–1253
28. Souza M, de Araujo D, Nassini R, Geppetti P, De Logu F (2020) TRPA1 as a therapeutic target for nociceptive pain. Expert Opin Ther Targets 24:997–1008
29. Sun W, Li C, Zhang Y, Jiang C, Zhai M, Zhou Q et al (2017) Gene expression changes of thermo-sensitive transient receptor potential channels in obese mice. Cell Biol Int 41:908–913
30. Tanioku T, Nishibata M, Tokinaga Y, Konno K, Watanabe M, Hemmi H et al (2022) Tmem45b is essential for inflammation- and tissue injury-induced mechanical pain hypersensitivity. Proc Natl Acad Sci U S A 119:e2121989119
31. Taylor B, Skorput AGJ, Gore R, Schorn R, Riedl MS, Marron Fernandez de Velasco E et al (2022) Targeting the somatosensory system with AAV9 and AAV2retro viral vectors. PLoS ONE 17:e0264938
32. Vulchanova L, Schuster DJ, Belur LR, Riedl MS, Podetz-Pedersen KM, Kitto KF et al (2010) Differential Adeno-Associated Virus mediated gene transfer to sensory neurons following Intrathecal delivery by direct lumbar puncture. Mol Pain 6:31
33. Wang S, Kobayashi K, Kogure Y, Yamanaka H, Yamamoto S, Yagi H et al (2018) Negative regulation of TRPA1 by AMPK in primary sensory neurons as a potential mechanism of painful Diabetic Neuropathy. Diabetes 67:98–109
34. Wei H, Koivisto A, Saarnilehto M, Chapman H, Kuokkanen K, Hao B et al (2011) Spinal transient receptor potential ankyrin 1 channel contributes to central pain hypersensitivity in various pathophysiological conditions in the rat. Pain 152:582–591
35. Wei H, Karimaa M, Korjamo T, Koivisto A, Pertovaara. A (2012) Transient receptor potential ankyrin 1 ion channel contributes to guarding pain and mechanical hypersensitivity in a rat model of postoperative pain. Anesthesiology 117:137–148
36. Wilson SR, Gerhold KA, Bifolck-Fisher A, Liu Q, Patel KN, Dong X et al (2011) TRPA1 is required for histamine-independent, mas-related G protein–coupled receptor–mediated itch. Nat Neurosci 14:595–602
37. Xie HJ, Li J, Lian N, Xie M, Wu MM, Tang K et al (2023) Defective branched-chain amino acid catabolism in dorsal root ganglia contributes to mechanical pain. EMBO Rep 24:e56958
38. Yang F, Sun W, Yang Y, Wang Y, Li CL, Fu H et al (2015) SDF1-CXCR4 signaling contributes to persistent pain and hypersensitivity via regulating excitability of primary nociceptive neurons: involvement of ERK-dependent Nav1.8 up-regulation. J Neuroinflammation 12:219
39. Yang OJ, Robilotto GL, Alom F, Alemán K, Devulapally K, Morris A et al (2023) Evaluating the transduction efficiency of systemically delivered AAV vectors in the rat nervous system. Front Neurosci 17:1001007
40. Yao CC, Sun RM, Yang Y, Zhou HY, Meng ZW, Chi R et al (2023) Accumulation of branched-chain amino acids reprograms glucose metabolism in CD8 + T cells with enhanced effector function and anti-tumor response. Cell Rep 42:112186
41. Yeh MC, Wu B, Li Y, Elahy M, Prado-Lourenco L, Sockler J et al (2021) BT2 suppresses human monocytic-endothelial cell adhesion, bone Erosion and inflammation. J Inflamm Res 14:1019–1028
42. Yin C, Liu B, Dong Z, Shi S, Peng C, Pan Y et al (2024) CXCL5 activates CXCR2 in nociceptive sensory neurons to drive joint pain and inflammation in experimental gouty arthritis. Nat Commun 15:3263
43. Zeng Z, Lan T, Wei Y, Wei X (2022) CCL5/CCR5 axis in human diseases and related treatments. Genes Dis 9:12–27
44. Zhang D, Zhao W, Liu J, Ou M, Liang P, Li J et al (2021) Sodium leak channel contributes to neuronal sensitization in neuropathic pain. Prog Neurobiol 202:102041
45. Zhang H, Wang C, Zhang K, Kamau PM, Luo A, Tian L et al (2022) The role of TRPA1 channels in thermosensation. Cell Insight 1:100059
46. Zhenyukh O, Civantos E, Ruiz-Ortega M, Sanchez MS, Vazquez C, Peiro C et al (2017) High concentration of branched-chain amino acids promotes oxidative stress, inflammation and migration of human peripheral blood mononuclear cells via mTORC1 activation. Free Radic Biol Med 104:165–177
47. Zhong S, Liu F, Giniatullin R, Jolkkonen J, Li Y, Zhou Z et al (2023) Blockade of CCR5 suppresses paclitaxel-induced peripheral neuropathic pain caused by increased deoxycholic acid. Cell Rep 42:113386
48. Zhou M, Lu G, Gao C, Wang Y, Sun H (2012) Tissue-specific and nutrient regulation of the branched-chain α-Keto acid dehydrogenase phosphatase, protein phosphatase 2Cm (PP2Cm). J Biol Chem 287:23397–23406

Publisher's note